GEOFISICA INTERNACIONAL

REVISTA DE LA UNION GEOFISICA MEXICANA, AUSPICIADA POR EL INSTITUTO DE GEOFISICA DE LA UNIVERSIDAD NACIONAL AUTONOMA DE MEXICO

Vol. 21 México, D. F., 1o. de abril de 1982 Núm.2

HARMONIC ANALYSIS OF THE ALBEDO AND LONGWAVE OUTGOING RADIATION FIELD IN THE SYSTEM EARTH–ATMOSPHERE

O. Y. KÄRNER*
O. A. AVASTE*
(Received: May 31, 1982)
(Accepted: Sept. 22, 1982)

RESUMEN

Se han utilizado para análisis armónico bidimensional los valores medios mensuales del albedo y de la radiación de onda larga emitida del sistema Tierra-Atmósfera. Las coordenadas son la latitud geográfica y el tiempo. Usando una malla de 2.5° se determinaron los coeficientes armónicos para 71 zonas latitudinales. Los datos primarios utilizados son tres años de mediciones de satélites NOAA (julio 1974 - junio 1977). Los resultados de los cálculos se analizaron agrupando los armónicos de la manera siguiente: dos grupos representando variabilidad espacio temporal independiente y un tercer grupo que tiene en cuenta esta variabilidad espacio temporal. El peso de los diferentes armónicos y grupos se estimó en términos de valores zonales anuales de la variación y las diferencias anuales en las amplitudes y fases de las armónicas.

* *W. Struve Astrophysical Observatory*
Tartu 202444, Toravere, Estonia, URSS.

ABSTRACT

The data on the monthly mean values of the albedo and the outgoing longwave radiation from the system Earth-atmosphere were subjected to a two-dimensional harmonic analysis. The coordinates were geographical latitude and time. Harmonic coefficients were found for 71 latitudinal zones with a width of 2.5°. The three-year NOAA satellite data (July 1974 - June 1977) served as primary data. The results of calculations were analysed while grouping harmonics as follows: two groups representing independent time and space variability; the third one took into consideration the temporal-spatial interdependent variability. The weight of different harmonics and groups were estimated in terms of yearly-zonal values of the variance and yearly differences in amplitudes and phases of harmonics.

The accuracy of the representation of the Earth-atmosphere energy balance was estimated on the basis of a few first harmonics.

INTRODUCTION

Satellite data on the albedo and on the outgoing radiation fields give new possibilities for the investigation of climatic trends. The aim of this paper is to analyse the variability of the above fields by using two-dimensional Fourier expansions with the intention of determining diagnostic expressions for boundary conditions, which could be used in numerical models for long-term weather forecasts as well as in the climate theory. Considering the above an attempt was made to investigate the disposition of the ridges of the Fourier harmonics above the globe and to compare them with the distribution of the real physical processes taking place in the atmosphere.

The analysis was made separately for all the three years (1974-1977). A yearly-zonal sample variance of the monthly mean values above the 2.5°x2.5° trapezoids serves as a measure of the variability of the albedo (a) and of the outgoing longwave radiation (D) fields. All amplitudes of harmonics are given as relative values A'_{jmn} showing the share they have in that variance, i.e.

$$A'_{jmn} = \frac{1}{2s_j^2} A^2_{jmn} \quad .$$

Calculations of the two-dimensional Fourier harmonics were carried out for all the latitudinal zones j for the albedo (α_{jik}) and for the outgoing longwave radiation (D_{jik}) by using Fourier expansions:

$$\hat{x}_{jik} = x_{joo} + \sum_{m=1}^{M} A_{jmo} \cos\left(\frac{m\pi k}{6} - \alpha_{jmo}\right) + \\ + \sum_{n=1}^{N} A_{jon} \cos\left(\frac{n\pi i}{72} - \alpha_{jon}\right) + \\ + \sum_{m=1}^{M} \sum_{n=1}^{N} \left\{A_{jmn} \cos\frac{m\pi k}{6} \cos\left(\frac{n\pi i}{72} - \alpha_{jmn}\right) + \right. \\ \left. + B_{jmn} \sin\frac{m\pi k}{6} \cos\left(\frac{n\pi i}{72} - \beta_{jmn}\right)\right\} . \qquad (1)$$

Here j = 1 . . . 71 while j = 1 designates the zone $87.5^{o} \div 90^{o}$N, i = 1 . . . 144 gives the longitudinal coordinate of the elementary trapezoid, e.g. i = 1 designates the 0–2.5^{o}E. The value k = 1 . . . 12, while k = 1 determines July. Coefficients in this expansion were calculated from the space-measured fields (α_{jik}) and (D_{jik}):

$$A_{jmn} = \mu_{m,n}\sqrt{a_{jmn}^2 + c_{jmn}^2} \qquad \alpha_{jmn} \text{ arc tan } \frac{c_{jmn}}{a_{jmn}}, \quad n > 0$$

$$A_{jmo} = \mu_{m,n}\sqrt{a_{jmo}^2 + b_{jmo}^2} \qquad \alpha_{jmo} = \text{arc tan } \frac{b_{jmo}}{\alpha_{jmo}}$$

$$B_{jmn} = \mu_{m,n}\sqrt{b_{jmn}^2 + d_{jmn}^2} \qquad \beta_{jmn} = \text{arc tan } \frac{d_{jmn}}{b_{jmn}}$$

$$a_{jmn} = \frac{1}{\pi^2} \sum_{k=1}^{12} \sum_{i=1}^{144} x_{jik} \cos\frac{m\pi k}{6} \cos\frac{n\pi i}{72} ,$$

$$b_{jmn} = \frac{1}{\pi^2} \sum_{k=1}^{12} \sum_{i=1}^{144} x_{jik} \sin\frac{m\pi k}{6} \cos\frac{n\pi i}{72} ,$$

$$C_{jmn} = \frac{1}{\pi^2} \sum_{k=1}^{12} \sum_{i=1}^{144} x_{jik} \cos\frac{m\pi k}{6} \sin\frac{n\pi i}{72} ,$$

$$d_{jmn} = \frac{1}{\pi^2} \sum_{k=1}^{12} \sum_{i=1}^{144} x_{jik} \sin\frac{m\pi k}{6} \sin\frac{n\pi i}{72} ,$$

$$x_{joo} = \frac{1}{4} \alpha_{joo}$$

$$\mu_{m,n} = \begin{cases} \frac{1}{2} & m > 0, \ n = 0 \quad \text{or} \quad m = 0, \ n > 0 \\ 1 & m > 0, \ n > 0. \end{cases}$$

When n = 0 the second term in formula (1) gives the temporal variability of the zonal mean values, we have the first group of harmonics. When m = 0 the second group of harmonics, represents the time-dependent interzonal variability. When $m \neq 0$, $n \neq 0$, the third group describes the variability which depends both on time and on the geographical coordinates.

It follows from the above that the harmonics of the first group represent primarily the effect of the changing declination angle of the Sun. The harmonics of the second group are connected with the distribution of the continents and the seas in the given latitudinal zone.

In this paper we shall take into account the harmonics which make up over 4 per cent of the total variance. This value (4 per cent) was chosen empirically, as the harmonics with smaller amplitudes have phases which change from year to year within wide limits.

PRIMARY DATA

The monthly mean fluxes emerging from the system Earth-atmosphere long-wave radiation (D_{jik}) and the albedo of the system Earth-atmosphere (α_{jik}) served as primary data for the present study. These values were determined on the basis of the scanning radiometer measurements carried out aboard the NOAA satellites (Gruber, 1978; Winston *et al.*, 1978). In this paper we used the data collected in the time-interval from July 1974 to June 1977. The coefficients of the Fourier expansion were calculated for three subintervals with a length of one year.

RESULTS

A) *Annual mean values and variances*

The annual mean values of the longwave outgoing radiation D_{joo} and of the albedo α_{joo} as well as the mean values for the total four-year period were published by Winston *et al.* (1979). The dispersion analysis showed that differences in the yearly mean values $\Delta D_{joo} = 2-5$ W/m^2 and for $\Delta\alpha_{joo} = 0.02-0.1$, were reliable on the 95 per cent significance level.

This means that year-to-year variations in the contemporary climate are significant when one tries to obtain a deeper insight into the admissibility of one or another process that may govern the regional (with a spatial scale of 1000 km) or the global climate. Table 1 presents the 3-year mean values for different latitudinal zones of $\bar{D}_{joo}$ and $\bar{\alpha}_{joo}$ deduced from the NOAA satellite data. These values correspond to the term x_{joo} in formula (1). We did not investigate the possible mistakes made in

Table 1

3-year Mean Values of D- and α-fields
according to zone-numbers

j	$\bar{D}_{j00}$	$\bar{\alpha}_{j00}$	j	$\bar{D}_{j00}$	$\bar{\alpha}_{j00}$	j	$\bar{D}_{j00}$	$\bar{\alpha}_{j00}$	j	$\bar{D}_{j00}$	$\bar{\alpha}_{j00}$
1	195	.40	19	242	.35	37	260	.26	55	228	.43
2	196	.41	20	246	.34	38	260	.26	56	224	.46
3	198	.41	21	249	.32	39	262	.26	57	222	.44
4	200	.43	22	253	.31	40	265	.25	58	218	.51
5	202	.44	23	259	.29	41	267	.25	59	215	.53
6	205	.49	24	264	.29	42	269	.25	60	211	.56
7	208	.47	25	270	.27	43	270	.25	61	208	.57
8	210	.46	26	273	.26	44	270	.25	62	204	.58
9	212	.54	27	275	.25	45	269	.26	63	198	.60
10	214	.51	28	275	.25	46	267	.26	64	189	.63
11	217	.51	29	274	.24	47	263	.27	65	179	.62
12	220	.46	30	271	.23	48	260	.28	66	170	.60
13	222	.44	31	266	.23	49	255	.30	67	164	.58
14	225	.43	32	260	.25	50	251	.32	68	161	.57
15	228	.42	33	254	.28	51	245	.34	69	160	.52
16	231	.40	34	253	.29	52	241	.36	70	158	.54
17	235	.38	35	257	.27	53	237	.38	71	150	.51
18	238	.37	36	260	.25	54	232	.40			

determining these values due to errors committed in intensity measurements or by the effect of the selected final atmospheric models, but we estimated only the mean latitudinal variability of the sample variances $s^2(D)$ and $s^2(\alpha)$. The results averaged over 3 years are illustrated in Fig. 1. The sample variance for the albedo $s^2(\alpha)$ is given with a scale factor of 10^4, i.e. it is multiplied by the value 10^4.

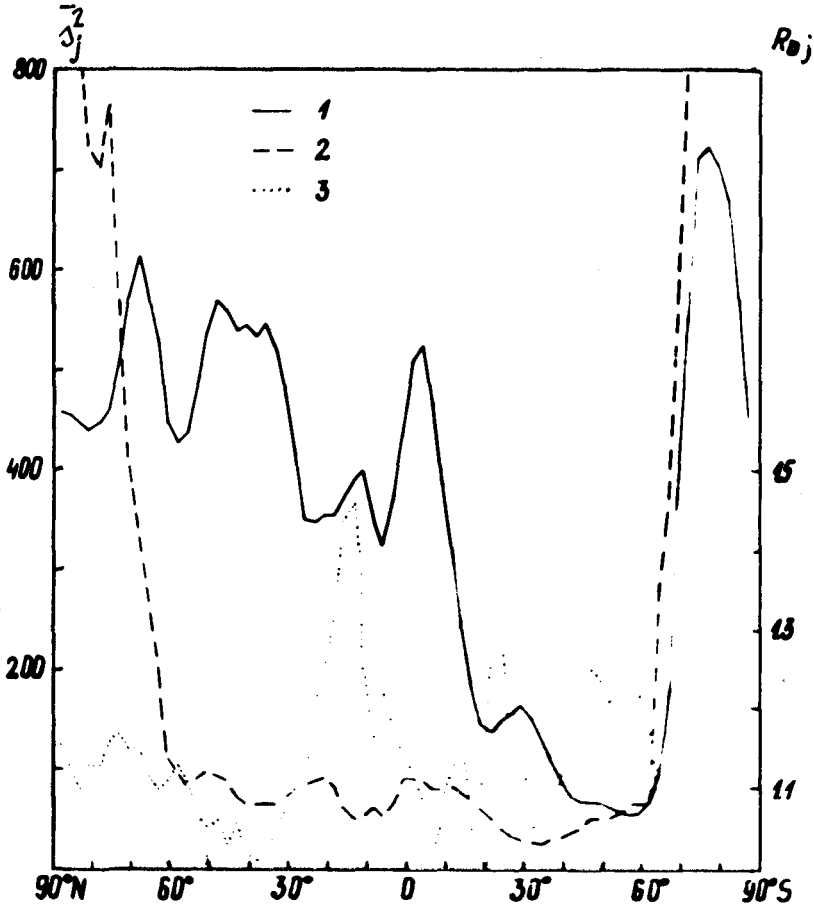

Fig. 1. The mean estimates of annual variances in different latitudinal zones: 1 - for outgoing thermal radiation, 2 - for albedo field (both given by left-side scale) and 3 - the ratio

$$R_{Dj} = \frac{s_j^2(D)_{max}}{s_j^2(D)_{min}}$$

(right-side scale).

B) *Year-to-year variations of variances*

We compare the ratio of the maximum variance to the minimum variance for three successive years 1974-1977, i.e.

$$R_{xj} = \frac{s^2_{j\,max}}{s^2_{j\,min}} \quad .$$

For the outgoing radiation the ratio R_{Dj} lies in the interval $1 \leqslant R_{Dj} \leqslant 1.20$ for most of the zones (see Fig. 1, right-side ordinate). In the selected three-year period (1974-1977) the data on D were more stable in the zone of $10^{o}-50^{o}$N and in the region south of the latitude 65^{o}S. In latitudinal zones of $10^{o}-20^{o}$N and $20^{o}-30^{o}$S the ratio R_{Dj} had values of 1.4 and 1.3 respectively.

For the albedo field there were three zones where $R_{\alpha j}$ had values higher than 1.2: in the latitudinal belts of $\varphi = 10^{o}-20^{o}$N, $55^{o}-65^{o}$N and in the region south of latitude 25^{o}S.

Nevertheless, it is not correct to assume that D - and α - fields are independent. In the case of independent normal samples with equal variances the critical value of $R_x(x = D, \alpha)$ at the 96 per cent significance level would be 1.10 (for samples with a volume equal to that of the experimental samples).

C) *Zonally mean temporal dependence*

Fig. 2 represents latitudinal variations of values $\bar{A}'_{j10}$ (part a) and $\bar{\alpha}_{j10}$ (part b) averaged over the three-year period which correspond to the outgoing radiation field (D) and to the albedo field (a). Relative values of amplitudes for the D-field are always higher than those for the α-field in all latitudinal zones except for two: 47^{o}, $5-62^{o}5$S and 67^{o}, $5-87^{o}$, 5S. Amplitudes of these harmonics (A_{j10}) "disappear" in the latitudinal zones $25^{o}-17^{o}$, 5N, $5^{o}-0^{o}$N and 17^{o}, $5-25^{o}$S, consequently in these zones there does not exist any temporal dependence in the D- and α-fields. It should be pointed out that these zones are closer to the tropic of Cancer, thermal equator and to the tropic of Capricorn, respectively. In the latitudinal zone $70^{o}-40^{o}$N amplitudes A_{j10} for D- and α-field are in opposite phases, i.e. increasing D-values correspond to decreasing α-values. This could be explained by the effect of snow in winter over continents and at the same time by increased amounts of clouds over the oceans on that latitudinal belt. Above the polar circle in both hemispheres the amplitudes A_{j10}(a) are close to zero.

Differences in phases for this harmonic between different years for the D-field in the northern hemisphere were as large as 0.15 and in the southern hemisphere

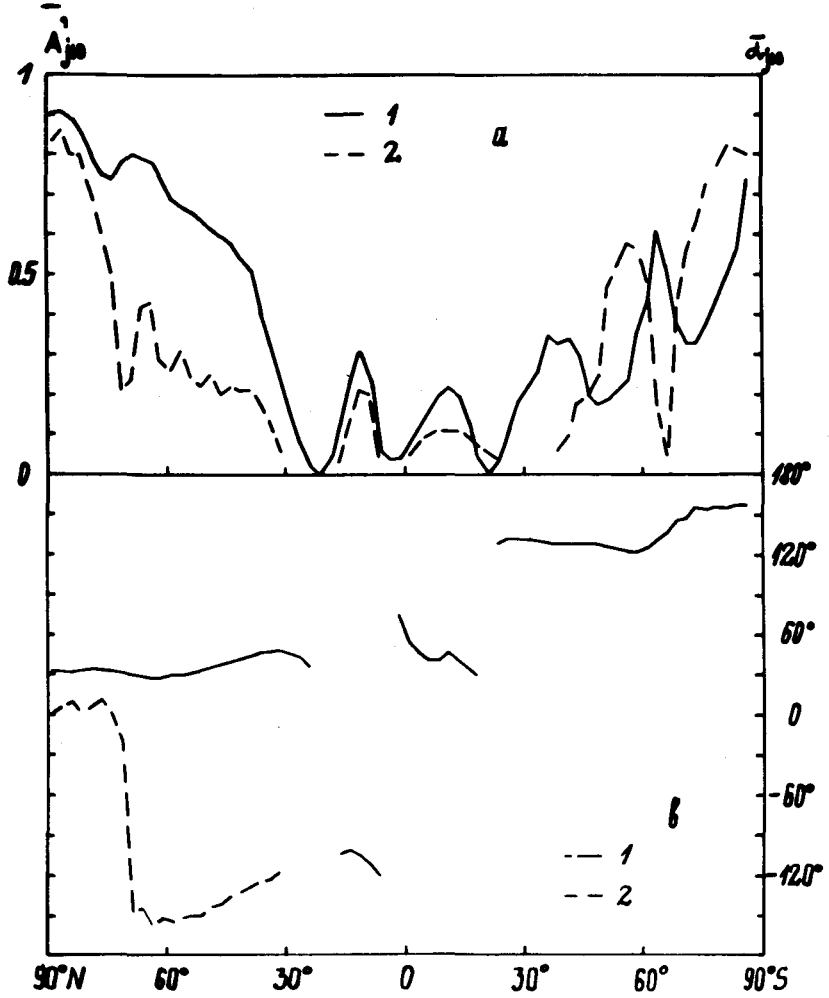

Fig. 2. The mean relative amplitude $\bar{A}'_{j10}$ (part a) and its phase (part b) of the annual harmonic for outgoing thermal radiation (1) and albedo (2) for different latitudinal zones.

−0.25, i.e. in time lapse it made 8 and 15 days, respectively. For the α-field these differences were significantly larger: the corresponding time lapse in the northern hemisphere was 15 days and in the southern hemisphere as large as 5 months. It follows from this that there is no sense in trying to determine the mean value for the phase angle α_{j10} of the albedo field, at least not in the latitudinal belt 20°–60°S.

Large variations in phase angles are connected with a high variability in the zonal mean cloud amounts, as these latitudinal zones are mainly covered by the oceans. The amplitudes A_{j20} are significantly different from zero only in polar regions.

At the same time there exists a significant difference in the yearly mean values of the two first years in relative amplitudes (see Table 2). In Table 2 the average amplitudes for the α-field in the region around the North Pole are determined from the three-year data, while in the region around the South Pole only the first-year data were usable as the albedo values of the two other year were erroneous because of technical problems (Winston *et al.*, 1978).

Table 2

Relative amplitudes and phases when m = 2, n = 0; $A'^{*}_{j20}(D)$ - the mean amplitude value deduced from the first two-year data; $A^{\circ}_{j20}(\alpha)$ the amplitude value deduced from the first year data

j	$A'^{*}_{j20}(D)$	$\alpha_{j20}(D)$	$A'_{j20}(\alpha)$	$\alpha_{j20}(\alpha)$	j	$A'_{j20}(D)$	$\alpha_{j20}(D)$	$A^{\circ}_{j20}(\alpha)$	$\alpha_{j20}(\alpha)$
1	.02	.98	.02	3.11				.31	.34
2	.03	.93	.05	−2.61	63	.04	.08	.06	−1.45
3	.02	.79	.10	−2.43	64	.04	.26	.29	.21
4	.01	.79	.13	−2.71	65	.04	.26	.29	.20
5			.15	−2.80	66	.05	.26	.27	.16
6			.23	−1.90	67	.07	.27	.19	.40
7			.25	−2.58	68	.09	.29	.26	.23
8			.31	−2.41	69	.10	.23	.06	.21
9			.10	− .92	70	.12	.23	.19	.64
10			+.18	−2.71	71	.15	.23	.05	.05

The D-field relative amplitudes A'_{j20}, which had been calculated from the data on July 1976 to June 1977, yielded values of 0.10, 0.08, 0.06, 0.04, when j = 1,.. 4. It follows from the data presented in Table 2 that these values were significantly higher than those deduced from the two first-year data-sets. In the amplitudes of the α-field such large discrepancies in year-to-year data did not exist. The above discussion demonstrates that because of year-to-year variations in primary data and in measuring accuracy problems there exist serious difficulties in a correct approximation of the D- and α-field over the whole globe.

It is possible that the increase in the mean effective temperature of the system Earth-atmosphere T_{eff} in the summer and winter seasons and the decrease of T_{eff}

in the spring and autumn seasons are connected with the special circulation El Niño, since at the same time there are no significant deviations in the temporal variations of the albedo in those zones. To have a more definite assurance for the above guess, a multi-year data-set and a more detailed study are needed.

Fig. 3 presents the total effect of the two harmonics which approximate the temporal variations, i.e. the values of $r_j = A'_{j10} + A'_{j20}$ for the D- and α-fields. Temporal variations of the α-field have amplitudes which are smaller than those of the

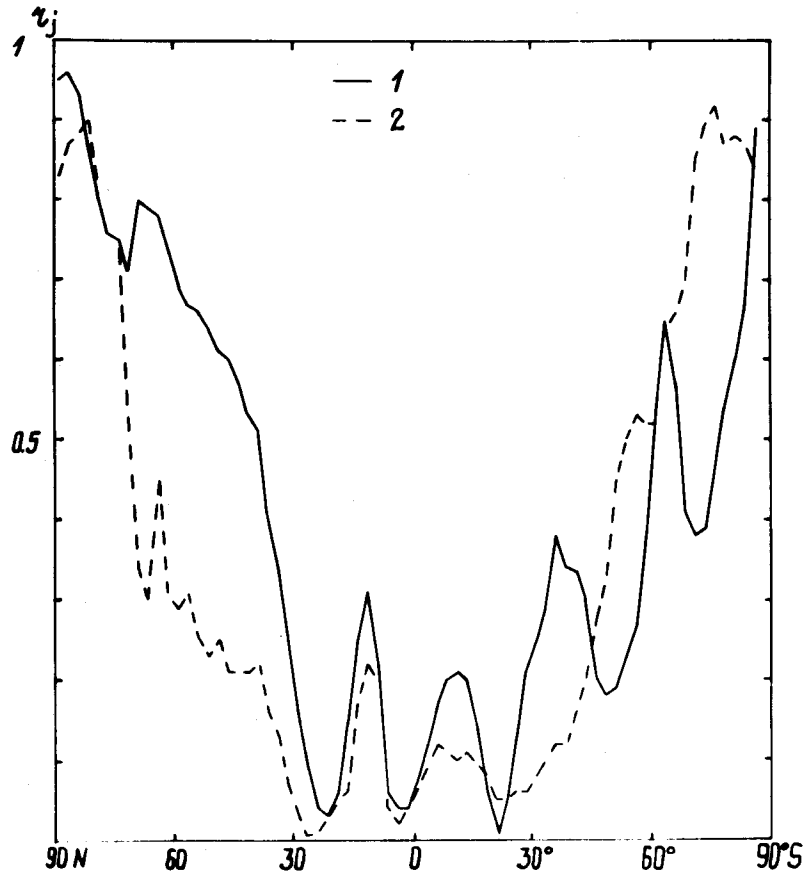

Fig. 3. The sum of the two first harmonics

$$(A_{j10}^2 + A_{j20}^2)/2s_j^2$$

in shares of variance for outgoing thermal radiation (1) and albedo (2) in different latitudinal zones.

D-field for all latitudes except for the zones south of 45°S. The small value of the amplitude $A_{j10}(D)$ over the latitude belt 70°S shows that there is a considerably smaller annual variation of D values than in the adjacent zones. In this zone the amplitudes $A_{j10}(D)$ have values comparable with the values $A_{j01}(D)$, i.e. in this zone the mean temporal variation is equal to the geographical variations connected with the asymmetry of the contour of the Antarctic. In the α-field variations the above minimum in the zone $\varphi = 70°S$ does not exist. It might be explained by the fact that in the summer season the low-level stratiform clouds exist over the climatic Antarctic frontal zone.

Summarizing the analysis of the two first temporal harmonics, it should be pointed out that the zonally mean annual variation describes the main bulk of the variations in the D- and α-fields only over the polar regions.

D) *Zonal variations ("standing waves")*

The harmonics of the second group represent time-independent variations, i.e. they give the interzonal anisotropy of the albedo and of the outgoing radiation fields. According to the definite zone, there may exist as many as five harmonics, which describe a still significant share in the spatial variations of these fields. The above-mentioned harmonics may have different values in different years. Let us study separately for all these harmonics the significance levels of the interzonal variations and the year-to-year variations. In Table 3 the mean relative amplitudes for the first three harmonics of this group for the D- and α-fields are presented. The phases of the harmonics (the position of ridges) with the wave numbers n = 1.2 are given in Fig.4, showing that there exists a large shift in the ridge in adjacent latitudinal zones when the amplitude values A_{jon} are small. When the j-value corresponds to the zone $\varphi = 60°N$, the amplitude for the albedo $A_{j01}(a)$ is significant but it does not coincide with the significant amplitude $A_{j01}(D)$. In the belt $\varphi = 30°-20°N$ both $A_{j01}(a)$, $A_{j01}(D)$ have maximum values, while their phases differ somewhat less than $\pi/2$, i.e. these harmonics have not been caused by the cloud cover. It is interesting that in the zone $\varphi = 15°-20°N$ $A_{j01}(a)$ and $A_{j01}(D)$ coincide in phases: their ridges are situated over the Sahara Desert. Over the Equator we have a secondary maximum of both the amplitudes $A_{j01}(a)$ and $A_{j01}(D)$, but there is a phase difference: the ridge in the D-field lies over Africa, but the ridge of the α-field is shifted towards the Pacific Ocean (approximately 10° from the coast of Peru). In the Southern Hemisphere there exists a maximum for the α-field in the zone 20°S, and another maximum for the D-field in the zone 30°S. As can be seen from Fig. 4a, the ridge of $\alpha_{j01}(D)$ lies over the Pacific and with an increasing latitude shifts from New Zealand to the Bellinghausen Sea and further to the South Pole.

Table 3

Relative amplitudes of D- and α-fields, when m = 0, n = 1.2 3

j	$\bar{A}'_{j01}(D)$	$\bar{A}'_{j02}(D)$	$\bar{A}'_{j03}(D)$	$\bar{A}'_{j01}(\alpha)$	$\bar{A}'_{j02}(\alpha)$	$\bar{A}'_{j03}(\alpha)$
1						
2						
3						
4			.01			
5	.02	.01	.03	.01		
6	.03	.03	.05	.01		
7	.03	.03	.02	.02	.01	.02
8	.01	.03	.02	.03	.02	.02
9	.01	.03	.01	.04	.03	.02
10	.02	.03		.06	.05	.02
11	.04	.02		.13	.03	.03
12	.04	.03		.22	.02	.06
13	.04	.03		.12	.06	.05
14	.04	.03		.07	.02	.07
15	.05	.03		.04	.01	.05
16	.05	.02		.02	.01	.05
17	.06	.03		.01	.02	.05
18	.08	.04		.04	.04	.04
19	.08	.04	.02	.07	.02	.13
20	.09	.05	.02	.06	.01	.16
21	.10	.05	.02	.10	.01	.09
22	.13	.09	.03	.13	.02	.03
23	.13	.13	.03	.14	.02	.03
24	.15	.16	.04	.16	.01	.19
25	.16	.16	.05	.14	.02	.22
26	.17	.14	.07	.09	.01	.27
27	.17	.12	.10	.09	.03	.29
28	.15	.12	.11	.10	.05	.23
29	.12	.11	.09	.09	.07	.25
30	.10	.09	.04	.03	.03	.25
31	.09	.05	.08	.01	--	.20
32	.07	.04	.07	.02	--	.07
33	10	.04	.04	.10	.02	.06

(Table 3, continued)

j	$\bar{A}'_{j01}(D)$	$\bar{A}'_{j02}(D)$	$\bar{A}'_{j03}(D)$	$\bar{A}'_{j01}(\alpha)$	$\bar{A}'_{j02}(\alpha)$	$\bar{A}'_{j03}(\alpha)$
34	.10	.14	.02	.09	.04	.04
35	.12	.19	.03	.08	.11	.09
36	.19	.21	.07	.08	.15	.11
37	.18	.21	.06	.07	.17	.12
38	.18	.19	.06	.06	.20	.11
39	.13	.15	.10	.04	.12	.15
40	.06	.09	.13	.04	.05	.11
41	.01	.05	.14	.07	.04	.09
42	.01	.04	.11	.10	.03	.06
43	.06	.03	.10	.14	.02	.06
44	.11	.04	.09	.14	.05	.06
45	.14	.05	.09	.13	.03	.03
46	.16	.06	.09	.11	.02	–
47	.17	.06	.10	.08	.01	.01
48	.17	.06	.09	.06	.02	.02
49	.14	.05	.07	.05	.01	.11
50	.11	.03	.09	.04	.02	.15
51	.07	.02	.06	.03	.02	.13
52	.04	.02	.05	.03	.09	.12
53	.09	.02	.04	.03	.05	.11
54	.19	.01	.04	.03	.07	.05
55	.33	.01	.03	.04	.04	.02
56	.41	.01	.02	.03	.03	.01
57	.47	–	.02	.03	.03	.01
58	.39	–	.02	.02	.03	–
59	.30	–	.02	.01	.03	–
60	.21	–	.04	.01	.03	–
61	.13	.01	.04	.01	–	–
62	.06	.02	.05	.01	–	–
63	.18	.08	.01	–	–	–
64	.35	.09	–	–	–	–
65	.43	.04	.05	–	–	–
66	.39	.02	.14	–	–	–
67	.35	.04	.09	–	–	–
68	.35	.04	.01	–	–	–
69	.32	.04	.01	–	–	–
70	.26	.01	.01	–	–	–
71	.07	–	–	–	–	–

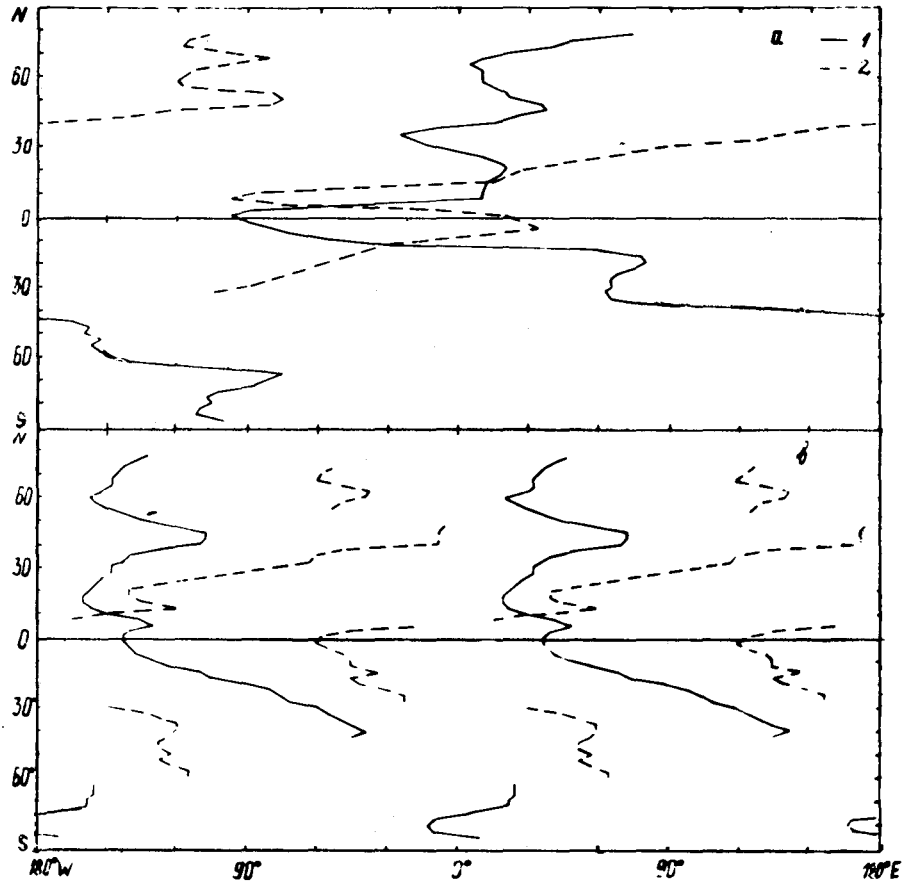

Fig. 4. The distribution of phases of two first harmonics $\bar{\alpha}_{j01}$ (part a), $\bar{\alpha}_{j02}$ (part b) for outgoing radiation (1) and albedo (2) versus latitude.

The ratio of the amplitudes of different years changes less than the variance in the given zone (see Fig. 1). If the given amplitude represents more than 15 per cent of the variance, then the year-to-year shift in its phase is less than 10^{o} for the D-field and less than 15^{o} for the α-field. If the given amplitude represents less than 5 per cent in the total variance, the year-to-year shift in phases could reach the value of $\pi/3$. An exception to this was observed empirically: in the period of 1976/1977 years in the zone $0-7.5^{o}$N the ridge α_{j01} (D) was shifted $\sim 40^{o}$ eastward, compared with its coordinate in the two previous years and in the zone $0^{o}-7.5^{o}$S its eastward shift was equal to 20^{o}. An analogous shift was observed for the same year also for the α-field: in the zone $0-10^{o}$N the ridge was 30^{o} eastward compared with the two

previous years. It is quite plausible to think that the above shifts were caused by "El Niño", i.e. by the warm ocean current in the equatorial zone of the Pacific Ocean (Namias, 1978).

The ridge $\alpha_{j02}(D)$ Fig. 4b with a considerable value of the amplitude shifts from the Pamirs towards the Libian Desert. After that it turns south-east, passes over the Somali Peninsula and follows the coastline up to the Equator, then it goes with southern ocean currents in the Indian Ocean to the southern coast of Australia. The second branch of this ridge stays over the Pacific Ocean. For the albedo-field the ridges of the harmonics $\alpha_{j02}(\alpha)$ with values of considerable amplitude lies over the

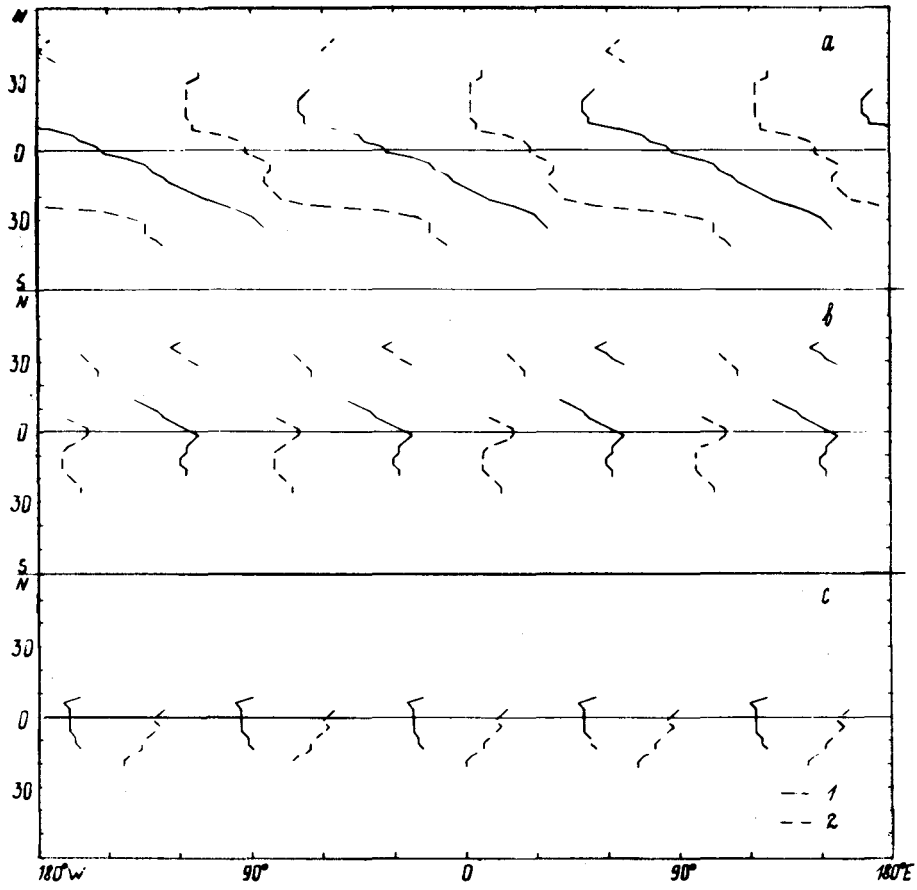

Fig. 5. The same as Fig. 4 for $\bar{\alpha}_{j03}$ (part a) $\bar{\alpha}_{j04}$ (part b) and α_{j05} (part c).

South American continent and over the Sunda Islands. The year-to-year changes in the phases $\alpha_{j02}(D)$ are similar to the changes in the $\alpha_{j01}(D)$ values in case these harmonics represent more than 5 per cent in the total variance. El Niño is traceable in the year-to-year changes of the phases $\alpha_{j02}(\alpha)$: in the years 1976/1977 in the zone 7.5°N–2.5°N the phase $\alpha_{j02}(\alpha)$ was shifted 50° eastward compared with the two previous years.

The distribution of the ridges of the harmonic n = 3 is given in Fig. 5a. In this case (n = 3) the harmonics of the D- and α-fields are in opposite phases. The ridges in the D-field move from the Arabic Peninsula towards the central part of Australia; across the Pacific and from the Bahamian Islands towards South Africa. The ridges with maximum amplitude values are observable over the central parts of the Atlantic, the Indian Ocean and in the Pacific approximately 5° eastward of the Tuamoto Archipelago. The respective ridges for the α-field $\alpha_{j03}(\alpha)$ pass over the central part of Africa, the eastern coast of China, the Philippines and Australia. Over the Pacific they are situated near the coast of America. Over the open oceans these ridges coincide with cloud clusters. The year-to-year variations of their phases can reach a value of 30° and this points out that such cloud clusters can exist over a given territory for a long period (comparable to years). In other regions the year-to-year changes in the phases of this harmonic have values of 5° for the D-field and 10° for the α-field.

The amplitudes of the harmonics n = 4 and n = 5 play a significant role only in a narrow belt from the Equator up to 30°S (see Table 4). The distribution of these ridges is given in Figs 5b and 5c respectively. The ridges $\alpha_{j04}(D)$ cross the Equator across the Indian Ocean (λ~65°E), Melanesia (155°E), the Pacific at ~115°W and the Atlantic at ~25°W. The ridges of $\alpha_{j05}(D)$ cross the Equator over the Indian Ocean (~50°E) (here runs the Australian current), the Sunda Islands (~120°E), the central part of the Pacific at λ = 170°W, and also at λ = 95°W as well as over the Atlantic at λ = 20°. Nearly all ridges are situated over the Oceans. For the albedo field the corresponding ridges lie over Africa, and its west coastline, goes across the Indian Ocean at λ = 100°E–110°E (the Malay Archipelago) lie over the central pacific (~160–170°W) and over the Western coast of South America. The ridges $\alpha_{j05}(\alpha)$ cross the Equator over Africa (~15°E), the Indian Ocean (~90°E), Melanesia (~160°E), the Pacific (~130°W), South America (~55°W). These ridges in the albedo-field are mainly controlled by the distribution of the continents in a given latitudinal zone. The total share of these five harmonics in variance is illustrated in Fig. 6. As can be seen from the above, there is no definite limit between the harmonics which describe the interzonal distributions "land-sea" and "clear-cloudy". Since cloud fields often cover coastal regions, the above two distributions partly coincide and their strict separation is not possible. It could be only pointed out that the spatial distribution of the two first harmonics (n = 1.2) is mainly determined by

Table 4

Relative amplitudes of the D- and α-fields when m = 0, n = 4,5

j	$\bar{A}'_{j04}(D)$	$\bar{A}'_{j04}(\alpha)$	$\bar{A}'_{j05}(D)$	$\bar{A}'_{j05}(\alpha)$
21	.01	.01		
22	.03	.02		.01
23	.04	.03		.02
24	.03	.07		.02
25	.02	.08		.02
26		.05		.02
27		.04		.02
28		.01		.01
29		.02		.04
30		.02		.03
31	.01	.01		
32	.02	.01		
33	.04	.02	.01	.01
34	.08	.09	.03	.01
35	.08	.12	.05	.02
36	.09	.15	.08	.05
37	.06	.11	.08	.08
38	.04	.06	.08	.06
39	.02	.09	.10	.05
40	.03	.11	.06	.04
41	.04	.14	.04	.04
42	.04	.15	.02	.03
43	.05	.20	.01	.02
44	.03	.21	–	.05
45	.02	.19	–	.03
46	.01	.15	–	.02
47	–	.08	–	.02
48	–	.02	–	.02

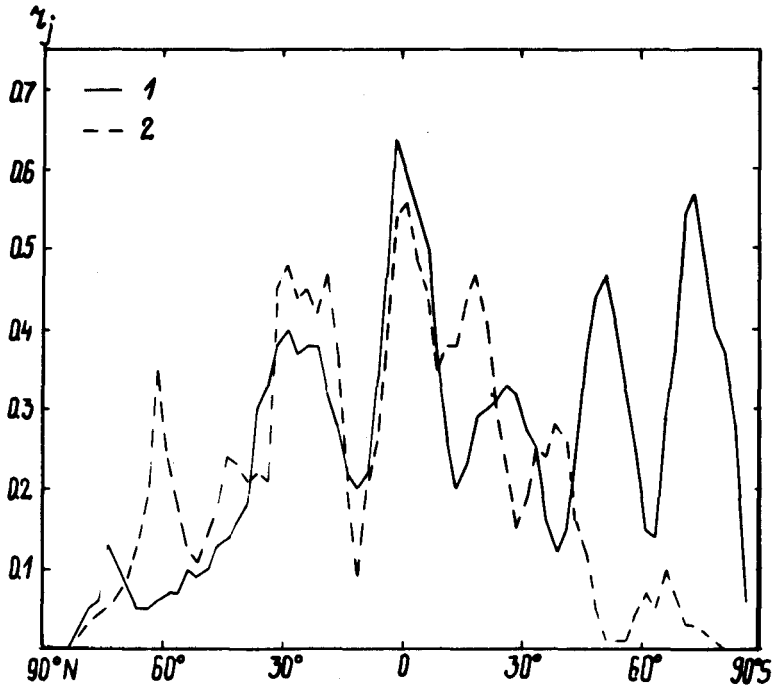

Fig. 6. The total weight in variance of the five time-independent harmonics

$$\left(r_j = \frac{1}{2s_j^2} \sum_{L=1}^{5} A_{jo1}^2 \right)$$

for outgoing radiation (1) and albedo (2) versus latitude.

the interzonal distribution "land-sea", while the three following harmonics (n = 3, 4, 5) are mainly dependent on the cloudfield distribution, as there exists for these harmonics a phase shift equal to $\pi/2$ between the D- and α-fields. It is worth to mention that for both fields (D and α) the ridges and troughs over the oceans of these five harmonics coincide with regions where according to the Programme "Profiles" by G. I. Marchuk (1979) are energetically active zones of the ocean-atmosphere interaction. It should be mentioned that the number of sites where the ridges and troughs of these first five harmonics lie are considerably higher than the number of the sites where G. I. Marchuk recommended to measure detailed profiles of the temperature fields of the sea and atmosphere and their energy exchange, with the aim of determining the advection of sensible heat in the ocean. The above harmonics describe variability in the effective radiation fields (shortwave and longwave), i.e. in the system atmosphere-underlying surface.

E) *"Moving waves"*

The harmonics of the third group are dependent on time (k) and space (i). They can be expressed as:

$$C_{jmn} \cos \left[\frac{n\pi i}{72} - \gamma_{jmn} \right] ,$$

where

$$C_{jmn} = \sqrt{A^2_{jmn} \cos^2 \left(\frac{m\pi k}{6} - \alpha_{jmn}\right) + B^2_{jmn} \cos^2 \left(\frac{m\pi k}{6} - \beta_{jmn}\right)} ,$$

$$\gamma_{jmn} = \arctan \frac{B_{jmn} \cos\left(\frac{m\pi k}{6} - \beta_{jmn}\right)}{A_{jmn} \cos\left(\frac{m\pi k}{6} - \alpha_{jmn}\right)} .$$

Therefore we have harmonics whose amplitudes and phases vary with time. Table 5 presents the relative amplitudes defined as

$$C'_{jmn} = \frac{A^2_{jmn} + B^2_{jmn}}{4s^2_j} ,$$

for the few first wavenumbers (m and n).

The three-year average arrangement of ridge for $\gamma_{j11}(D)$ in July, September and November is given in Fig. 7a. As can be seen from Table 5: this harmonic presents a comparatively smooth wave (the maximum amplitude covers 10 per cent of the variance) and it moves in summer and winter with a low speed. As a rule, its speed is higher (in spring and autumn) when its amplitude is at its minimum (it constitutes less than 1 per cent of the variance). Let us study this harmonic in three latitudinal zones, where its amplitude has a maximum. In the zone 45°–55°N this wave covers 6 per cent of the variance and moves eastward with a speed of up to 15° per month. Its ridge passes in summer through the Northern part of Kazakhstan and in winter moves from the Pacific towards the western coast of Canada. The next zone with a considerable amplitude for $C_{j11}(D)$ is 30°N–15°N. In summertime its ridge is situated over North Africa. The wave-front of this harmonic moves to NNW with a speed of 100 km per month. In winter it moves over the Pacific. Amplitudes are minimal in October and April. The third zone under consideration is in the zone 5°–10°S. This wave makes 5 per cent of the total variance and represents a vortex whose center moves in June to November over the Timor Sea and is from December to May over Brazil. It should be mentioned that year-to-year

Table 5

Relative amplitudes of D- and α-fields, when m = 1, n = 1, 2, 4

j	$\bar{C}'_{j11}(D)$	$\bar{C}'_{j11}(\alpha)$	$\bar{C}'_{j12}(D)$	$\bar{C}'_{j12}(\alpha)$	$\bar{C}'_{j14}(D)$	$\bar{C}'_{j14}(\alpha)$
12	.04	.02	.03			
13	.03		.06	.05		
14	.05	.02	.07	.13		
15	.06	.02	.08	.18		
16	.05	.02	.09	.23		
17	.06	.05	.10	.23		
18	.04	.06	.10	.23		
19	.02	.08	.08	.12		
20	.02	.08	.07	.04		
21	.02	.04	.07			
22	.03	.03	.05			
23	.06	.01	.05			
24	.07		.05	.02		
25	.07		.06	.03		
26	.07		.11	.04		
27	.08	.02	.14	.04		.03
28	.10	.02	.14	.03	.03	.03
29	.10	.04	.14	.04	.05	.03
30	.07	.07	.08	.05	.06	.05
31	.03	.06	.03	–	.07	.06
32	.03	.06	.03	–	.07	.06
33	.03	.05	.01	–	.05	.07
34	.04	.05	.04	.04	.03	.07
35	.04	.03	.06	.07	.03	.05
36	.02	–	.08	.05	–	.04
37	.02	–	.05	.03	–	.03
38	.01	.02	.04	–	.02	.04
39	.01	.03	.03	–	.05	.09
40	.03	.05	.02	–	.08	.10
41	.04	.05	.02	–	.09	.09
42	.06	.06	.02	–	.09	.06
43	.04	.05	.04	–	.08	.03
44	.03	.03	.03	–	.06	–
45	.04	.01	.04	–	.02	–

variations of this harmonics in the above zones are less than 2 per cent of the total variance, but the phase differences reach values up to 25°.

The respective harmonic for the α-field in Fig. 7b also shows considerable amplitudes in the above zones. In the zone 40–50°N in summer (June to September) there forms a vortex over the Pacific and it moves in winter across the Atlantic. In the zone 5–15°N in summer there originates a vortex over the Indian Ocean near

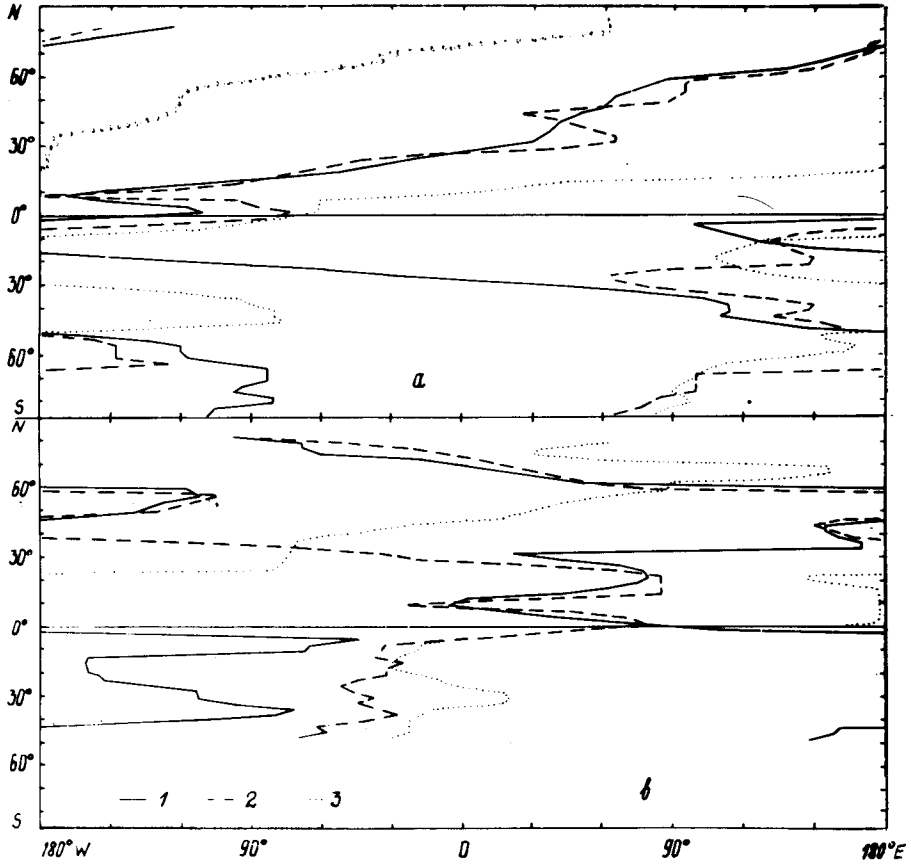

Fig. 7. Spatial distribution of the phase angle $\bar{\gamma}_{j11}$ in July (1), September (2) and November (3) for outgoing radiation (part a) and albedo (part b).

the coast of India, but in winter it forms over the eastern part of the Pacific. In the zone 10–15°S the amplitude over the Atlantic has considerable values in autumn and in spring then the ridge lies over the Atlantic and over the Coral Sea, respectively. For the α-field the year-to-year variations of amplitudes and phases are compar-

able with those in the case of the D-field. The waves with wavenumbers m = 1, n = 2 for the D-field in Fig. 8a are standing waves in winter over the Gulf Stream and Kuro Shio (from November to March). In summer the ridge γ_{j12}(D) in the zone 40°–15°N approximately coincides with the ridge of the wave α_{j02}(D). The coincidence of these two ridges is especially good over the African deserts. The second ridge of this wave lies over the Pacific and approximately coincides with the region of small cloudiness (Avaste *et al.*, 1979; Miller and Feddes, 1971).

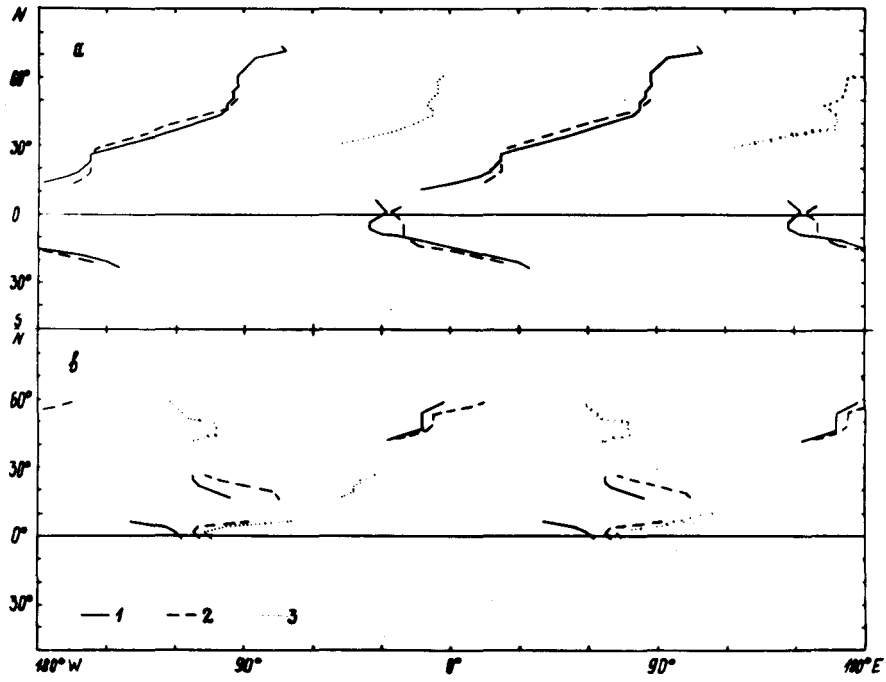

Fig. 8. Spatial distribution of the phase angle $\bar{\gamma}_{j12}$ in July (1), September (2) and November (3) for outgoing radiation (part a) and albedo (part b).

The respective wave in the α-field (the ridges presented in Fig. 8b) corresponds to the distribution of the snowcover in the zone 60°–42°, 5N. The ridges in winter "stand" nearly at longitude 75°E (i.e. on the line Omsk-Alma Ata), and 105°N (i.e. the eastern slopes of the Rocky Mountains). The rather high amplitude values of this harmonic indicate the limits with a permanent snowcover in the winter season. In summer the ridges of this harmonic "stand" over the Atlantic some degrees west of England, over the Pacific several degrees from the Kamchatka and the Kuril Islands. The average eastward speed of the ridge of this harmonic (in winter and summer) in the above latitudinal zone is 2.5° per month. The year-to-year differences in phases are up to 10° for months with high amplitudes.

The next wave, which has a considerably high amplitude, bears wavenumbers m = 1, n = 4. In some latitudinal zones it constitutes up to 10 per cent of the total variance (for both the D- and α-fields). The distribution of the ridges of this wave over one fourth of the Earth, corresponding to the Eastern Pacific in July, September and November, is presented in Fig. 9. In Fig. 9, it is possible to distinguish two steps in the movement of this wave: the first one corresponds to two first years in our analysis when in summer the eastward speed is small but amplitudes are rather large. The speed is 1-2° per month for both the D- and α-fields. The wave-speed increases towards the Equator. In the autumn of this step the wavespeed increases, but amplitudes decrease.

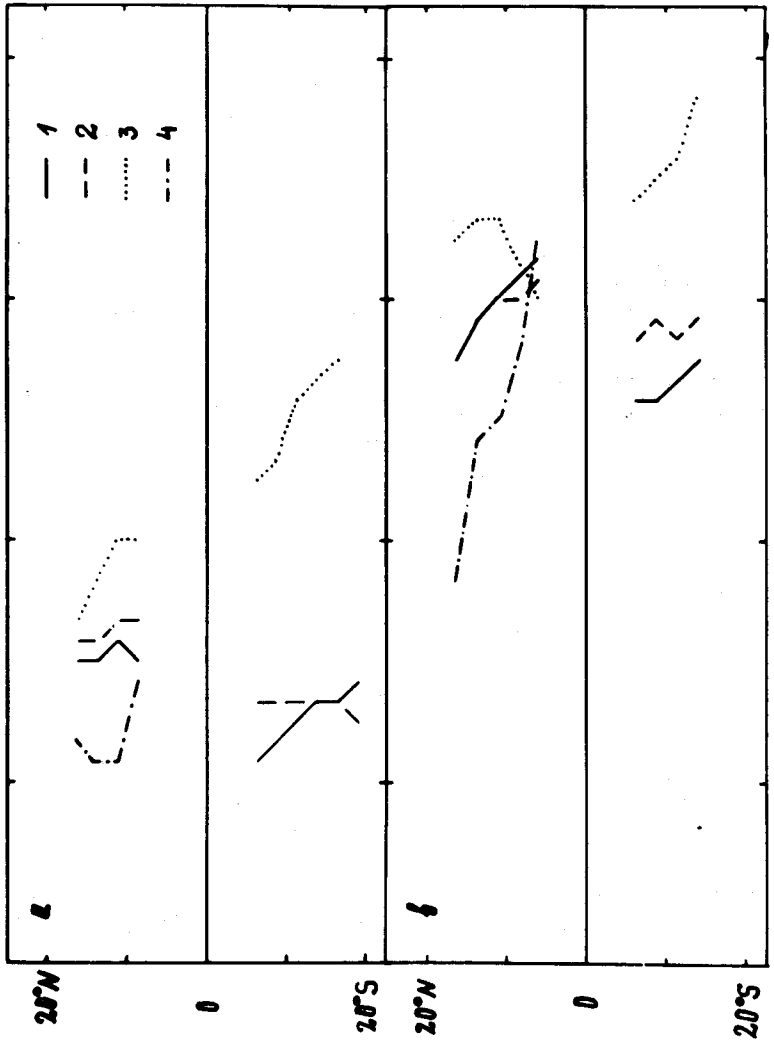

Fig. 9. The distribution of phase γ_{j14} on the one fourth of the Earth in the "unperturbed years" in July (1), September (2) and November (3) for outgoing radiation (a) and albedo (b). Curve 4 represents phase γ_{j14} in November in case of El Niño.

The second step in the movement of this wave is observable in the data of the third year starting from October 1976 the direction of the movement changes in the latitudinal belt 5–15°N, 25° for the D-field and ~30° for the α-field. In November the ridges are situated westward compared with the two previous years: approximately in the Southern Hemisphere we did not find such a deviation in the movement of this wave.

It should be pointed out that for both the D- and α-fields, the smallest amplitudes occur from November to December and from May to June; the largest amplitudes occur from August to September and from February to March. Taking into consideration the arrangement of the ridges of this wave, we concluded that the above peculiarities are connected with "El Niño".

The individual contribution of an harmonic with higher wave-number can in some latitudinal zones give only less than 4 per cent of the total variance.

The ridges of the harmonics of the third group lie mainly over the regions where for most of the time of a given month the weather is governed by anticyclons (the regions where there are ridges in the D-field) or - in the case of cyclons (the regions where there occur ridges in the α-field). It is possible to determine the mean speed of these vortices. The "vortex" of these waves for the D-field lies in summer over the continents, in winter - over the open oceans. In summer this coincides with higher temperatures over the continents. The "vortex" for the α-field "stands" mainly over the sea close to the coastal line. The main bulk of the waves of the third group has maximum amplitudes in summer and in winter. The only exception is $C_{j11}(\alpha)$, where the maximum amplitude occurs in the zone 5°–10°S (j = 42–44) in spring, the ridge is over the Atlantic near the eastern coast of Brazil and in autumn - the ridge is over the Coral Sea.

CONCLUSIONS

The harmonic analysis of the temporal-spatial fields of the outgoing thermal radiation (D-field) and the albedo (α-field) showed that when one distinguishes three groups of harmonics, it is possible to study the main temporal peculiarities and the interzonal spatial variabilities. Taking into consideration the mean zonal-spatial variances calculated from the data covering three successive years (1974-1977) it was shown that the first ten harmonics (divided into groups: 2÷3÷5) in a D-field approximation described the main bulk of the variances (see Fig. 10), there exist. If we take into account two temporal harmonics (m = 1, m = 2), five time-independent harmonics (standing waves) n = 1÷5 and three harmonics which describe the main moving waves (m = 1, n = 1; m = 1, n = 2; m = 1, n = 4), then for the D-field the largest residual variance remains in the zone 10°N–10°S, where the residual

variance is approximately 200 W^2/m^4. For the α-field the same number of harmonics leave the largest residual variance (0.02) in the zones 70–80°N and 70–80°S. Nevertheless, it should be pointed out that in the tropical zone the residual or "noise" amplitude is higher than any individual harmonic amplitude. This is valid for both the D- and α-fields.

The year-to-year changes of these ten harmonic amplitudes reach values constituting up to 10 per cent of the variance (for example A_{j20} near the North Pole). The year-to-year changes in the phases of the same harmonics can, for some latitudinal zone, be significant. This effect is probably connected with "El Niño" circulation type.

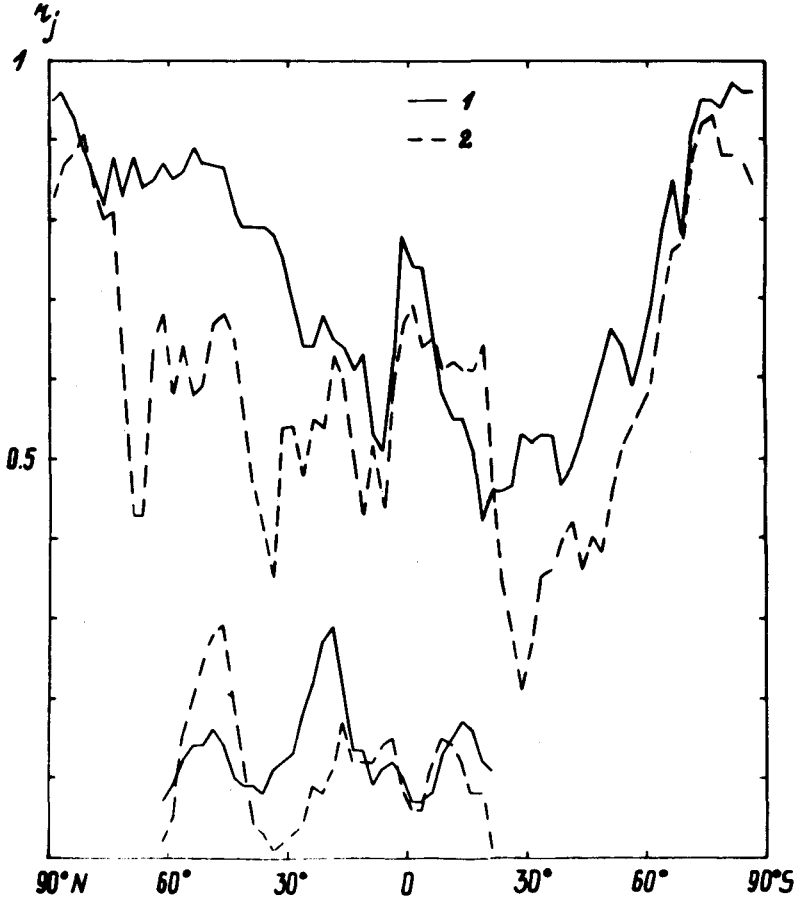

Fig. 10. The total weight of 10 main harmonics analysed in this paper and the total weight of the three harmonics (C_{j11}, C_{j12}, C_{j14}) calculated by formula $r_j = \frac{1}{4s^2}(C_{j11}^2 + C_{j12}^2 + C_{j14}^2)$ (presented in lower part of this Figure). Curves 1 denote harmonics for outgoing radiation, curves 2 - these for albedo.

When one tries to approximate the radiation budget, it should be mentioned that even the small variances in the albedo-field can cause large errors in approximating the radiation budget distributions. The shortwave radiation absorbed in the system "Earth-atmosphere" is equal to $J = S_0(1-\alpha)$, where S_0 is the flux of solar radiation incident on the upper boundary of the atmosphere. This equation allows us to estimate the variance of the J-field. For example, in the equatorial zone, where S_0 has an approximately constant value $\sim 400 W/m^2$ the variance of the absorbed flux is three times higher than the variance for the outgoing thermal flux. From here it follows that it is possible to approximate the shortwave radiation flux with the same accuracy as the longwave outgoing flux only when the α-field is approximated with correspondingly higher accuracy. This is a very strong demand. In practice the accuracy for the D-field is lower than for the α-field when we use an equal number of harmonics (Fig. 10). This must be considered in analysing the values of the radiation budget. The accuracy of the albedo field determines the accuracy of the radiation budget approximation over the greater part of the Earth.

BIBLIOGRAPHY

AVASTE, O. A., G. G. CAMPBELL, S. K. COX, D. DE MASTERS, O.U.KARNER, K. S. SHIFRIN, E. A. SMITH, E. J. STEINER, T. H. VONDER HAAR, 1979. On the estimation of cloud amount distribution above the World Oceans. Colorado State University. Atmos. Sci. Pap. No. 309, 73 pp.

GRUBER, A., 1978. Determination of the earth-atmosphere radiation budget from NOAA Satellite data. NOAA Technical Report NESS 76, Washington, D. C.

MARCHUK, G. I., 1979. Climate change modelling and the long-range problem of weather prediction. *Meteorologia i gidrologia No. 7,* 25-36. (in Russian).

MILLER, D. B., R. G. FEDDES, 1971. Global Atlas of Relative Cloud Cover 1967-1970. Washington, D. C., 236 pp.

NAMIAS, J., 1978. Multiple Causes of the North American Abnormal Winter 1976-1977. *Mon. Wea. Rev. 106,* 3, 279-295.

WINSTON, J. S., A. GRUBER, T. J. GRAY, Jr., M. S. VARNADORE, C. L. EARNEST and L. P. MANELLO, 1979. Earth-Atmosphere Radiation Budget analysis Derived from NOAA Satellite Data June 1974-February 1978, Vol. I, II. Meteorological Satellite Laboratory. Washington, D. C.